© Pol J Radiol 2020; 85: e144-e154
DOI: https://doi.org/10.5114/pjr.2020.93714

Received: 24.12.2019
Accepted: 10.02.2020
Published: 12.03.2020

Polish Journal of Radiology

http://www.polradiol.com

Original paper

Aftermath of pulmonary tuberculosis: computed tomography assessment

Sneha Satish Deshpande[A,B,C,D,E,F], Anagha Rajeev Joshi[A,B,C,D,E,F], Ankita Shah[A,B,C,D,E,F]

Lokmanya Tilak Municipal Medical College and General Hospital, Mumbai, India

Abstract

Purpose: Pulmonary tuberculosis (PTB) has clinically significant sequelae, even after recommended treatment completion. It is important to recognise these sequelae for accurate assessment of severity and treatment planning, if indicated.

Material and methods: We retrospectively analysed contrast-enhanced computed tomography (CT) scans of chest of 100 patients with previous history of treated pulmonary tuberculosis, excluding those with active pulmonary disease. CT findings were analysed based on parenchymal, airway, pleural, mediastinal, and vascular sequelae of PTB.

Results: Parenchymal sequelae included fibrosis with architectural distortion and volume loss (90%), cavities (21%) (with aspergillomas noted in 19% of these cases), and tuberculomas (54%). Airway involvement was noted as bronchiectasis (77%) and bronchial stenosis (4%) but none with broncholithiasis. Mediastinal sequelae included lymph node calcification (74%), fibrosing mediastinitis (1%), and pericardial tuberculosis (2%). Pleural sequelae included pleural thickening (22%), with 40.9% of these patients showing calcifications, and one patient with chronic chylous pleural effusion. Vascular sequelae included Rasmussen aneurysms (4%), enlarged bronchial arteries (3%), and systemic bronchial collaterals in 1% of our patients.

Conclusions: PTB has multiple appalling sequelae, which require due attention and appropriate treatment in symptomatic cases. Radiological evaluation forms an integral part in patient assessment and decision making.

Key words: pulmonary tuberculosis sequelae, cavities, tuberculoma, pleural thickening, Rasmussen's aneurysm.

Introduction

Pulmonary tuberculosis (PTB) contributes largely to the world health burden, not only due to the morbidity and mortality associated with active disease but also the morbidity associated with its sequelae [1-3]. Incidence of pulmonary tuberculosis is on the rise, with associated under-nutrition, diabetes, increasing prevalence of immunosuppression associated with AIDS, immunosuppressant drugs used with cancer chemotherapy or transplants, etc. Variable degree of drug resistance, non-compliance to treatment due to the long duration and various complications of the therapy has further added to the predicament [1-4]. All this has created a large group of patients who suffer from the various sequelae of pulmonary tuberculosis due to involvement of the airway, parenchyma, pleura, or pulmonary vasculature [5,6]. It is imperative to know about these sequelae of pulmonary tuberculosis to evaluate the severity of involvement and assess their contribution to the patients' symptoms and treatment planning, if indicated. We assessed the imaging features of sequelae of pulmonary tuberculosis in patients who presented with pulmonary symptoms, excluding those with active pulmonary disease.

Material and methods

Subjects

The study was started after approval from the Institutional Review Board. We conducted a retrospective observa-

Correspondence address:
Dr. Anagha Rajeev Joshi, Lokmanya Tilak Municipal Medical College and General Hospital, Mumbai, India, e-mail: anaghajoshi2405@gmail.com

Authors' contribution:
A Study design · **B** Data collection · **C** Statistical analysis · **D** Data interpretation · **E** Manuscript preparation · **F** Literature search · **G** Funds collection

tional study of contrast-enhanced computed tomography (CT) scans of 100 patients referred to our department over a period of one year (from January 2018 to December 2018) with previous history of pulmonary tuberculosis, treated based on standard recommendations, and presenting with pulmonary complaints like dyspnoea, cough, expectoration, haemoptysis, etc. Patients below 18 years of age and those with clinical, radiological, or microbiological evidence of active pulmonary tuberculosis were excluded from the study.

Scanning parameters

CT scans of the chest were performed as a part of routine diagnostic work on a 64-slice multiple detector computed tomography (MDCT) scanner (Philips Brilliance, Philips Medical Systems) after taking informed consent from the patients with no change in the hospital protocol.

Images were acquired in thin collimation depending on the phase. Image reconstruction was carried out on a Terarecon Aquarius workstation. Axial images were reconstructed using a slice thickness of 2.5 mm and 2.5 mm reconstruction increment, thinner if necessary, and viewed at standard soft tissue window settings. The scans were independently reviewed by two radiologists, and any disagreement was resolved by combined review of the scans and a consensus was reached.

Multi-detector computed tomography evaluation

CT findings were analysed based on parenchymal, airway, pleural, mediastinal, and vascular sequelae of tuberculosis. Parenchymal sequelae were classified as fibrosis with architectural distortion and volume loss, cavities, and tuberculomas. Fibrosis was objectively graded in each lung as follows: involving less than the volume of a bronchopulmonary segment as 1 point; and involving an entire volume of a segment as 2 points. Each lung involvement was graded accordingly with maximum points of the right lung being 20 and left lung being 16. Cavities were studied based on the number (single or multiple) and the thickness of the cavity wall, wall enhancement, and calcification. Complications like aspergillomas or bronchogenic carcinoma were noted.

Airway involvement was studied on the basis of bronchiectasis with its types and extent, bronchial stenosis, and broncholithiasis. Mediastinal sequelae included lymph node calcification, fibrosing mediastinitis, and pericardial tuberculosis.

Pleural sequelae include pleural thickening, which was evaluated on the basis of pleural thickness, enhancement, and calcification. Fibrothorax was characterised by diffuse pleural thickening with or without calcification and is frequently associated with volume loss of the affected hemithorax.

Vascular sequelae that were studied included Rasmussen aneurysms, enlarged bronchial arteries, and vasculitis leading to thrombosis.

Statistical analysis

Data was analysed using Statistical Package for Social Sciences (SPSS) version 17.0 for Windows (SPSS, Chicago IL, U.S.A). Mean and standard deviation were calculated for continuous variables. Proportions and frequency tables were used to analyse categorical variables.

Results

We retrospectively analysed contrast-enhanced CT scans of the chest in 100 patients with previous history of treated pulmonary tuberculosis, with a mean age of 50.7 ±1.8 years (18-85 years). Of these patients, 48 were males (48%) and 52 (52%) were females.

CT findings were analysed based on parenchymal, airway, pleural, mediastinal, and vascular sequelae of tuberculosis.

Ninety patients (90%) presented with parenchymal fibrosis, architectural distortion (Figure 1), and associated volume loss; with the commonest pattern of involvement being bilateral upper lobes (32/90 [35.56%]). The volume of lung involvement was objectively graded, and the mean score of parenchymal involvement was 9.3 ±4.4 (range, 2-20). Bronchogenic carcinoma was not noted in any of our patients.

Cavities were seen in 21 patients (21%), with 10/21 patients (47.62%) showing a single cavity (Figure 2) and 11/21 patients (52.38%) showing multiple cavities. All patients with solitary cavities showed associated parenchymal fibrosis (10/10, 100%), while 8/10 (80%) showed tuberculomas with calcification. Also, solitary cavities were more commonly seen in upper lobes (9/10, 90%), with only one patient showing a solitary healed cavity in the superior segment of the right lower lobe (1/10, 10%). The average wall thickness of the cavities was 2.9 ±0.7 mm (2-4 mm). All the cavities showed smooth non-enhancing walls. Solitary cavities most commonly showed upper lobe distribution, while when the cavities were multiple, other lobes were involved, including superior segments of bilateral lower lobes and right middle lobe. Aspergillomas were noted in 4/21 patients with pulmonary cavities (19%) (Figure 3), all the aspergillomas being in the upper lobes.

Tuberculomas were noted in 54 patients (54%), being bilateral in 41/54 patients (75.92%) and unilateral in 13 patients (24.07%). 48/54 patients (88.89%) showed calcified tuberculomas (Figure 4), while 6/54 patients (11.11%) showed only non-calcified tuberculomas. All these six patients, however, showed other sequelae of healed tuberculosis such as fibrosis or bronchiectasis. The pattern of calcification was diffuse (44/48 [91.67%]) and central (4/48 [8.33%]). The average size of the tuberculoma was 6 mm ±1.6 mm (3-10 mm). Enhancement of the nodules was assessed, with none of the tuberculomas in our patients showing enhancement.

Airway involvement was studied on the basis of bronchiectasis with its type and extent, bronchial stenosis, and

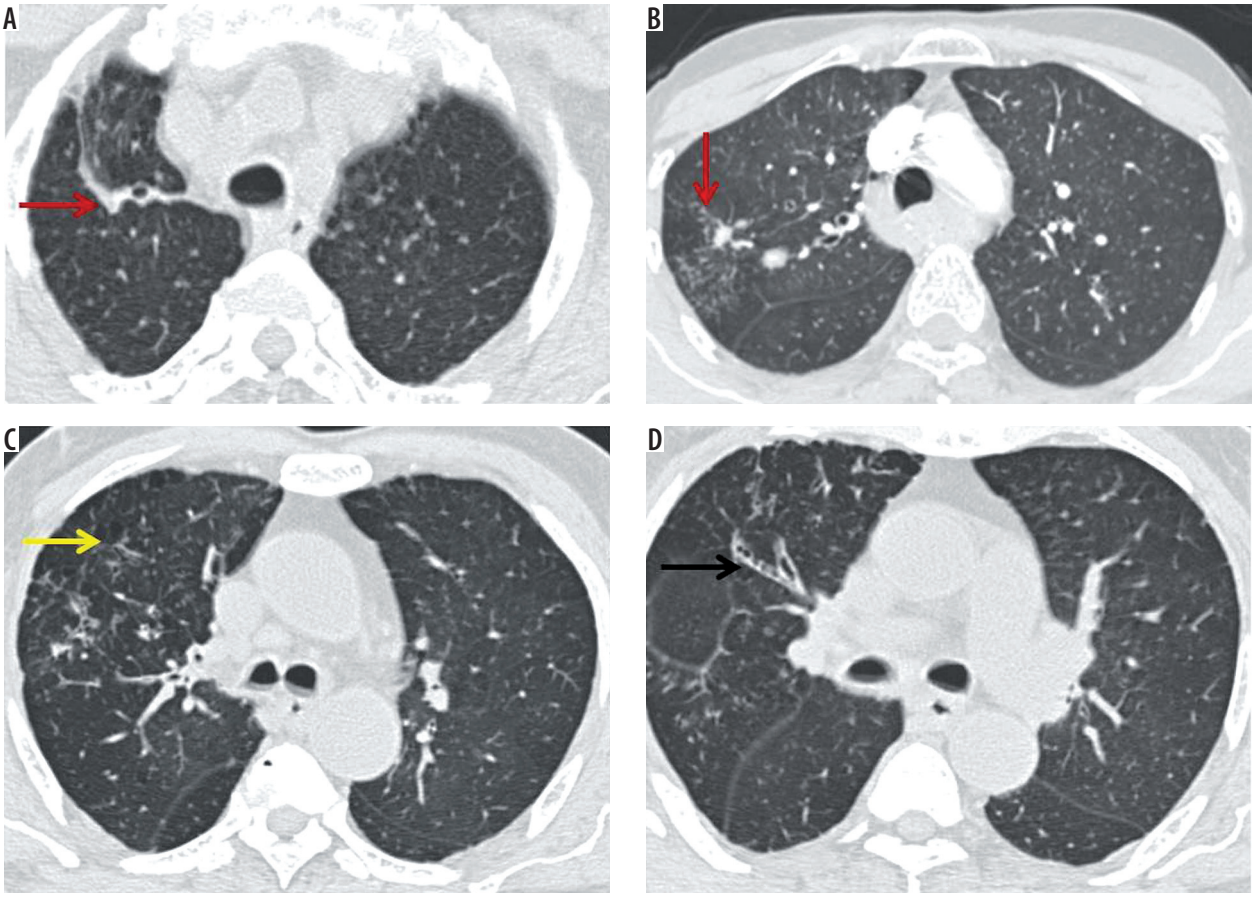

Figure 1. **A)** Fibrosis with architectural distortion (red arrow) involving the right upper lobe reaching up to the pleura associated with pleural thickening. **B)** Tuberculoma in right upper lobe with adjacent fibrosis reaching the major fissure and **(C)** associated emphysema and **(D)** bronchiectasis

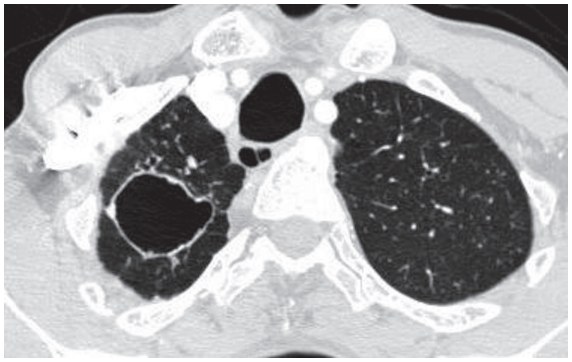

Figure 2. Thin-walled, well-defined cavity in the right upper lobe with mild right-sided volume loss

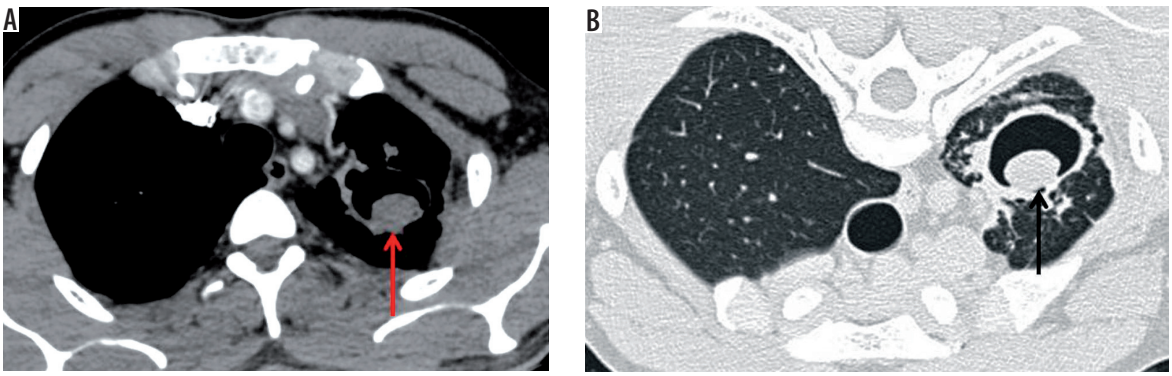

Figure 3. **A)** Aspergilloma with air crescent sign in a thin-walled cavity in the left upper lobe, which shows with adjacent fibrosis and associated left-sided volume loss. **B)** The aspergilloma shows change of position to dependent aspect on prone scan

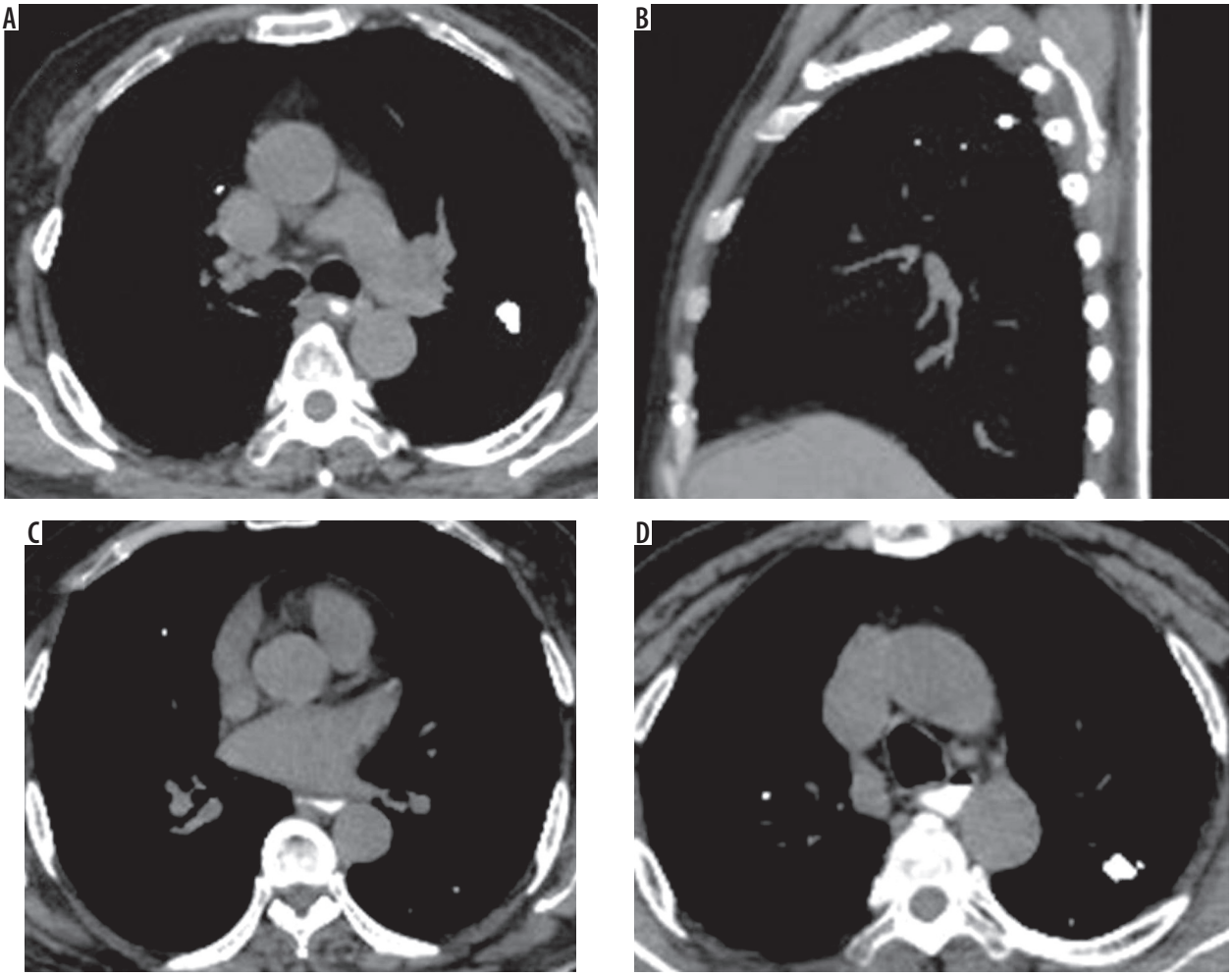

Figure 4. **A-D)** Axial plain chest computed tomography image mediastinal window showing multiple calcified nodules in both lungs showing diffuse calcification suggesting benign aetiology

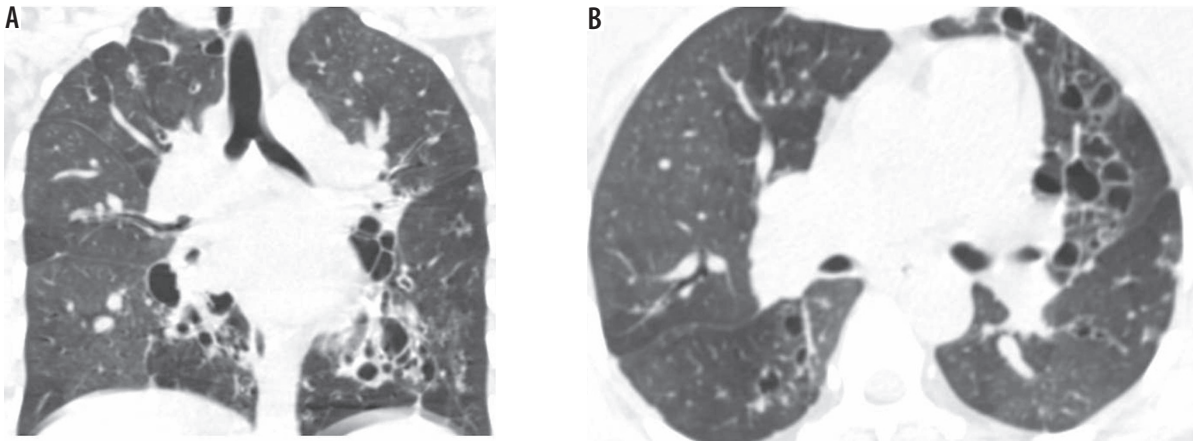

Figure 5. **A)** Coronal and **(B)** axial computed tomography lung window images showing varicose and cystic bronchiectasis in both lungs as a sequela of tuberculosis

broncholithiasis. Bronchiectasis was noted in 77 patients (77%), with 31/77 (40.26%) showing tubular bronchiectasis, 8/77 (10.39%) showing varicose bronchiectasis, and 38/77 (49.35%) showing cystic bronchiectasis (Figures 5 and 6). Four patients (4%) showed bronchial stenosis with distal collapse with fluid bronchogram, two of them involving the entire lung (Figure 7). The collapsed lung showed multiple areas of parenchymal calcifications. None of the patients in our series showed broncholithiasis.

Mediastinal sequelae included lymph node calcification, fibrosing mediastinitis, and pericardial tuberculosis. Calcified nodes were noted in 74 patients (74%) primarily

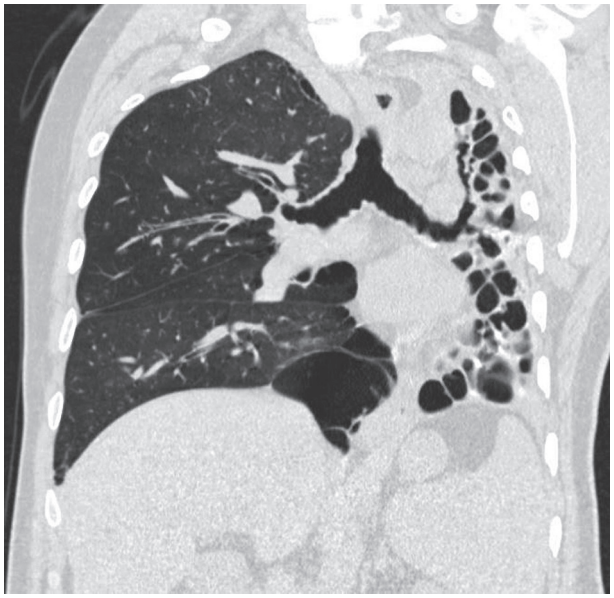

Figure 6. Coronal computed tomography lung window images showing cystic bronchiectasis with collapse of the entire left lung as a sequela of tuberculosis

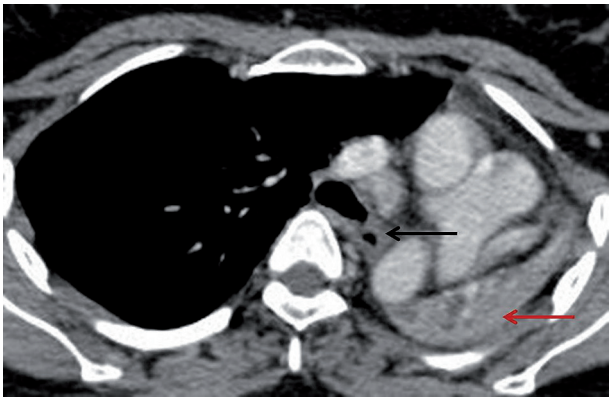

Figure 7. Axial post-contrast chest computed tomography image mediastinal window showing complete collapse of the left lung (red arrow). The left main bronchus shows wall thickening and luminal narrowing (black arrow)

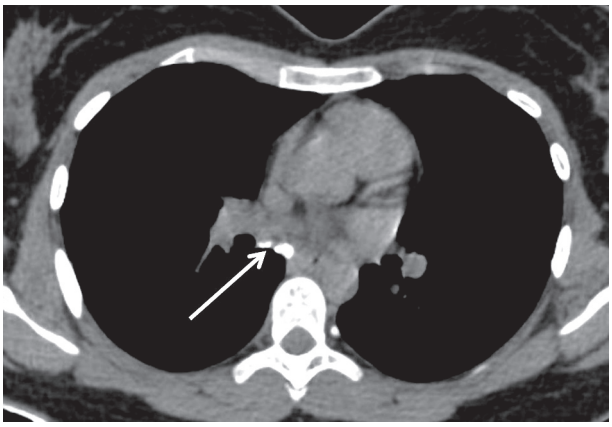

Figure 8. Plain axial computed tomography mediastinal window image showing calcified sub-carinal nodes (white arrow)

in pretracheal, paratracheal, precarinal, subcarinal, and hilar regions (Figure 8). Twi patients (2%) showed pericardial calcifications, who presented with constrictive pericarditis (Figure 9). One patient in our series presented with fibrosing mediastinitis, with severe narrowing of the right main pulmonary artery (Figure 10).

Pleural sequelae included pleural thickening, which was evaluated on the basis of pleural thickness, enhancement, and calcification. Pleural thickening was noted in 22 patients (22%), with the average pleural thickness being 3.3 ±1.04 mm (range, 2-7 mm) (Figure 11). 15/22 (68.18%) patients showed no pleural enhancement, while 7/22 (31.81%) showed mild pleural enhancement. No pleural nodularity was noted. 9/22 patients with pleural thickening (40.9%) showed interrupted calcifications (Figure 12). In our series, two patients (2%) showed continuous thick sheet-like calcification. One patient in our series presented with chronic pleural effusion with fat flu-

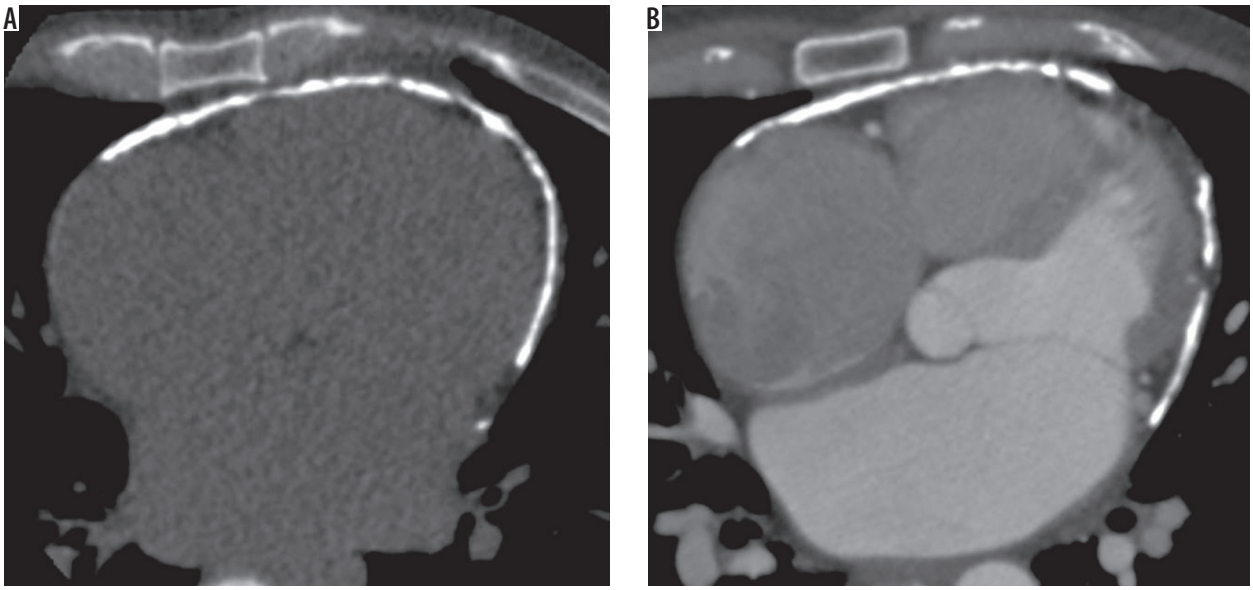

Figure 9. **A)** Plain **(B)** post-contrast axial computed tomography image showing pericardial calcification

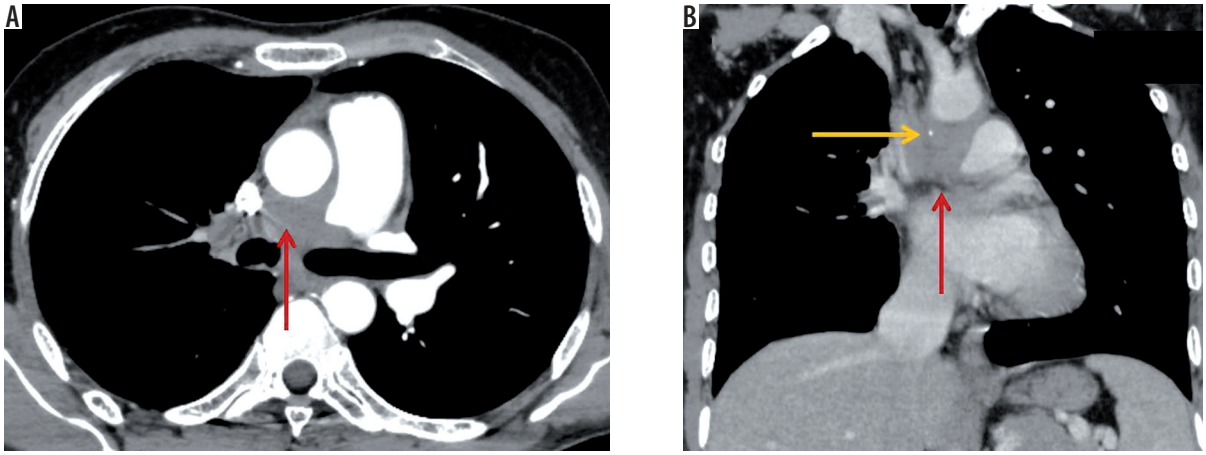

Figure 10. A 55-year-old male patient previously diagnosed with tuberculosis involving mediastinal nodes, presented with progressive dyspnoea. **A)** Axial and **(B)** coronal post contrast computed tomography image mediastinal window in a showing an ill-defined soft tissue density mildly homogenously enhancing mediastinal lesion along the right pulmonary artery completely encasing the artery and causing luminal obliteration (red arrow). It shows a focus of calcification (yellow arrow)

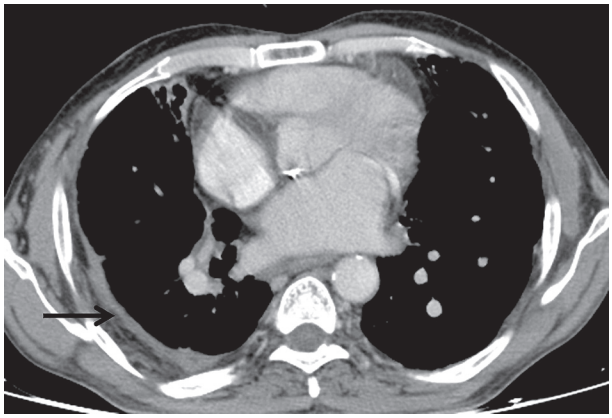

Figure 11. Axial post-contrast chest computed tomography image mediastinal window showing enhancing smooth pleural thickening involving the right costal pleura (black arrow)

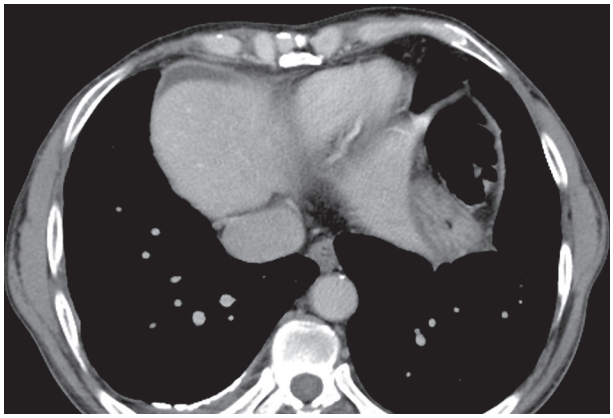

Figure 12. Axial post-contrast chest computed tomography image mediastinal window showing enhancing smooth pleural thickening with continuous sheet-like calcification (black arrow)

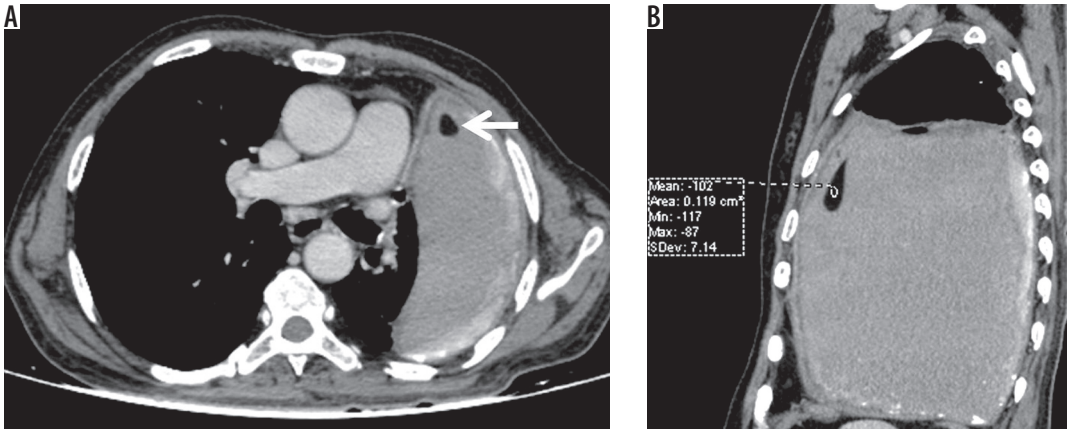

Figure 13. **A)** Axial **(B)** coronal post-contrast chest computed tomography image mediastinal window showing left-sided chronic pleural effusion with enhancing smooth pleural thickening and calcification. Fat-fluid level is noted in the pleural effusion (HU: -102). Chylous pleural effusion was noted on pleural fluid evaluation

id level suggesting chylous pleural effusion (Figure 13), which was proven on biochemical evaluation of pleural fluid.

Vascular sequelae that were studied included Rasmussen aneurysms, enlarged bronchial arteries, vascular thrombosis due to vasculitis, and systemic bronchial col-

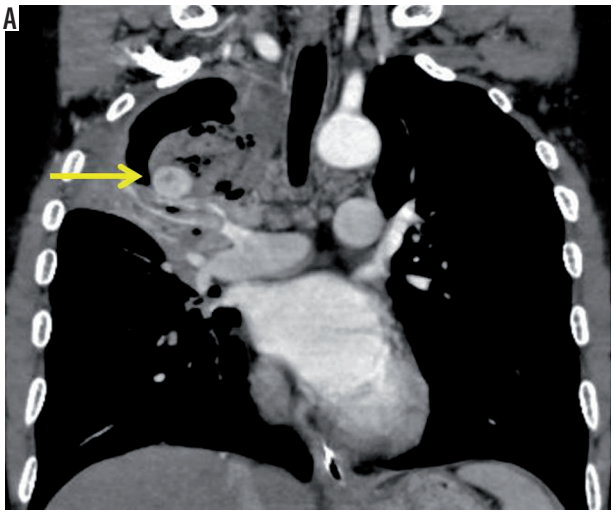

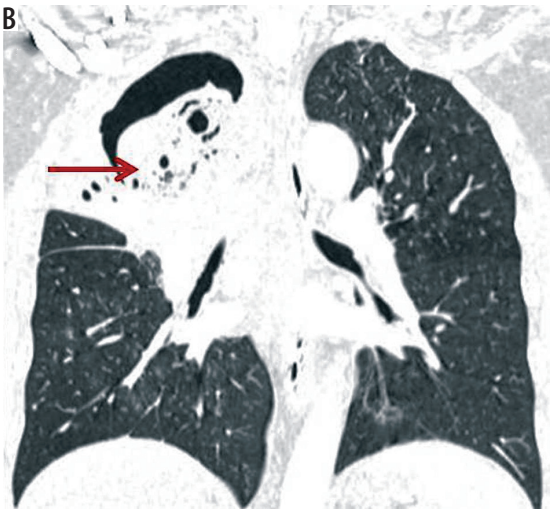

Figure 14. A 51-year-old male patient, previously treated for pulmonary tuberculosis, presented to the emergency services with chronic cough with multiple episodes of streaky haemoptysis followed by one episode of severe haemoptysis. **A)** Coronal post-contrast computed tomography image mediastinal window shows a large cavity in the right upper lobe with collapse of the right lung. A Rasmussen aneurysm (yellow arrow) is noted along the inferior wall of the cavity. Air crescent sign is seen in the cavity, which is also visible on **(B)** coronal lung window image (red arrow). This appearance may be seen in aspergilloma or a haematoma in the cavity in the presence of Rasmussen's aneurysm

laterals. Rasmussen's aneurysm was noted in four patients (4%), with the average size being 5 mm (Figure 14). Enlarged bronchial arteries were noted in three (3%) patients (Figure 15). No case of vascular thrombosis due to vasculitis was noted in our study. Systemic bronchial collaterals were noted in one of the patients in our series, with systemic collaterals noted from internal mammary artery, inferior phrenic artery, posterior intercostal arteries, and left gastric artery (Figure 16).

Discussion

Pulmonary sequelae of tuberculosis may lead to significant patient morbidity even after complete recommended therapy. It requires specifically targeted therapy based on the spectrum of involvement and its severity, with the treatment being mostly symptom targeted. Presentations like severe haemoptysis, fibrothorax, aspergilloma, etc. may require interventions. Our study population comprised 100 patients (mean age 50.7 ±1.8 years [18-85 years]) who had completed treatment for pulmonary tuberculosis according to standard recommended protocols, excluding those with documented active disease. They were symptomatic with pulmonary symptoms like dyspnoea, chest pain, haemoptysis, etc. for which they were referred to our department for CT scan of the thorax. CT findings were analysed based on parenchymal, airway, pleural, mediastinal, and vascular sequelae of tuberculosis.

Lung parenchymal lesions

Cicatrisation and destruction of the lung

Cicatrisation with atelectasis is seen commonly in healed post-primary tuberculosis, which may present as marked

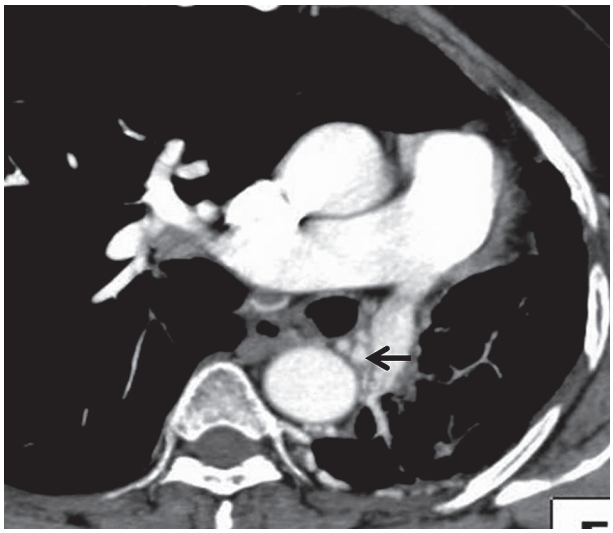

Figure 15. Axial post-contrast chest computed tomography image mediastinal window showing left-sided volume loss due to collapse of the left lung. There is hypertrophy of the bronchial arteries (black arrow)

'nonspecific pattern' of fibrosis consisting of parenchymal bands with architectural distortion and volume loss. There may be associated retraction of the hilum, mediastinal shift, pulling up of the diaphragm, and compensatory hyperinflation of the normal lung segments [5-7]. Apical pleural thickening associated with fibrosis and proliferation of extrapleural fat is commonly seen. Combinations of parenchymal and airway involvement may lead to complete destruction of a lung or a major part of a lung in the end stages of tuberculosis.

Ninety patients (90%) in our series presented with parenchymal fibrosis, architectural distortion, and associated volume loss, being the commonest presentation in our series. The commonest distribution of abnormalities was bilateral upper lobes (32/90 [35.56%]), which is consistent

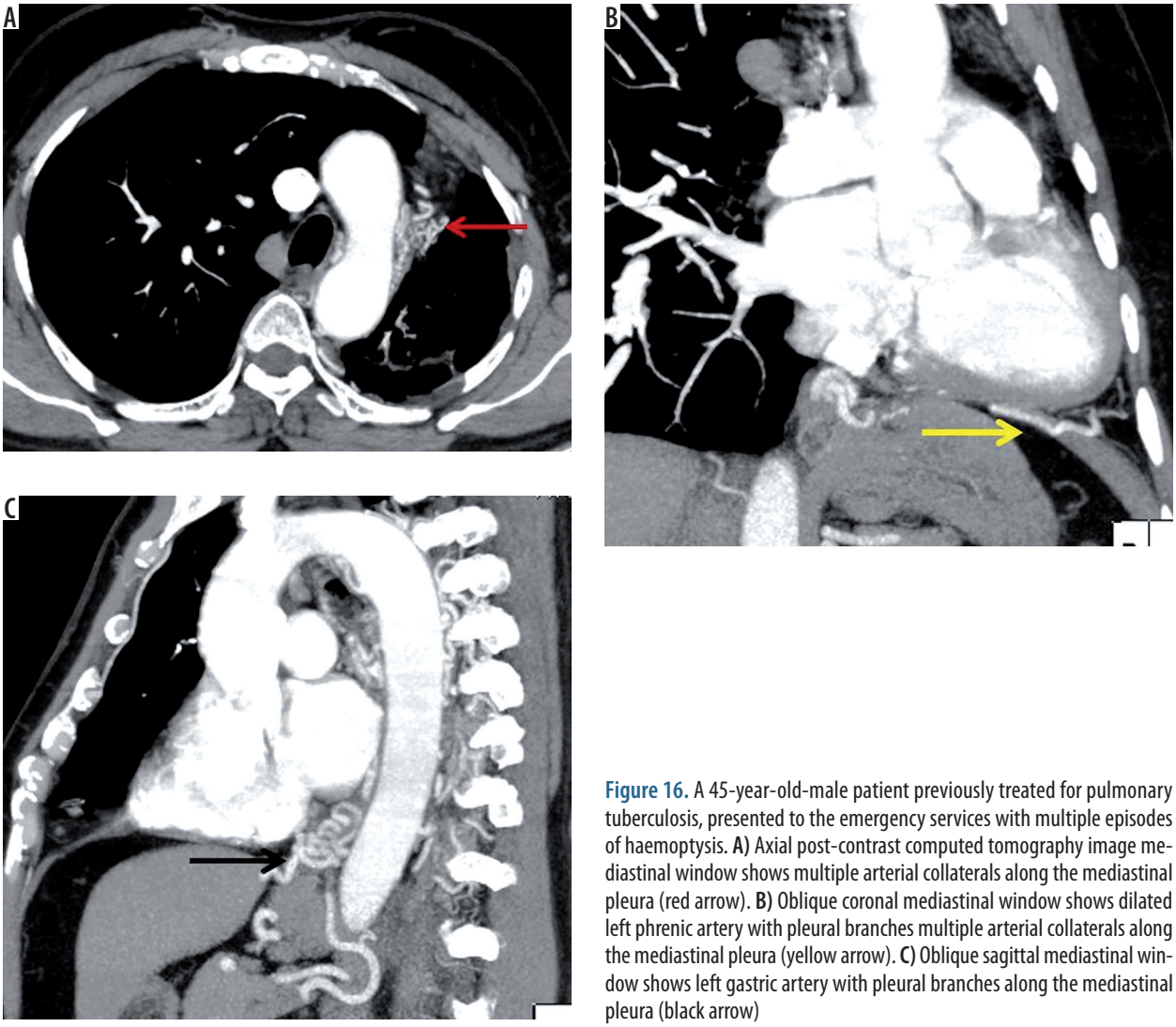

Figure 16. A 45-year-old-male patient previously treated for pulmonary tuberculosis, presented to the emergency services with multiple episodes of haemoptysis. **A)** Axial post-contrast computed tomography image mediastinal window shows multiple arterial collaterals along the mediastinal pleura (red arrow). **B)** Oblique coronal mediastinal window shows dilated left phrenic artery with pleural branches multiple arterial collaterals along the mediastinal pleura (yellow arrow). **C)** Oblique sagittal mediastinal window shows left gastric artery with pleural branches along the mediastinal pleura (black arrow)

with the predilection of upper lobes in post-primary tuberculosis (TB). Hatipoglu *et al.* [8] evaluated the high resolution computer tomography (HRCT) finding in patients with pulmonary tuberculosis and assessed 34 patients with inactive pulmonary tuberculosis. They found that HRCT scans showed fibrotic lesions (n = 34 [100%]), distortion of bronchovascular structures (n = 32 [94%]), and bronchiectasis (n = 24 [71%]) in patients with inactive tuberculosis. This is consistent with the proportion found in our study.

The volume of lung involvement was objectively graded, and the mean score of parenchymal involvement was 9.3 ±4.4 (range, 2-20). This underlines the grave effects of pulmonary tuberculosis on lung parenchyma and the impact it can have on lung function.

Cavities

Parenchymal cavities are one of the commonest presentations of active post-primary pulmonary tuberculosis. Tuberculous cavities heal by two processes: open and closed, depending upon the state of the draining bronchus [9]. In the open form of healing the lumen of the draining bronchus remains patent, the walls of the cavity become free of tubercle bacilli, usually in response to therapy, and the cavity wall undergoes fibrosis with subsequent epithelialisation. The cavity becomes thin walled because of regression of the pericavitary inflammatory reaction, and the fibrous walls contract, leading to a residual saccule opening into a bronchus. In the closed type of healing, the draining bronchus becomes occluded and the cavity either undergoes atelectasis and scar formation or the cavity becomes inspissated, leading to the appearance of pulmonary nodule or tuberculoma [6,10].

In our study, cavities were seen in 21 patients (21%), with 10/21 patients (47.62%) showing a single cavity and 11/21 patients (52.38%) showing multiple cavities. Patients presenting with solitary cavities showed upper lobe predominance, associated parenchymal fibrosis, and tuberculomas with calcification, which indicated previous tuberculous aetiology. Patients presenting with multiple parenchymal cavities showed upper lobe involvement in all cases, with associated involvement of other lobes.

The average wall thickness of the cavities in our study was 2.9 ±0.7 mm (2-4 mm), with all the cavities showing

smooth non-enhancing walls. Thin-walled, healed tuberculous cavities may mimic bullae, cysts, or pneumatoceles when the bronchial communication is not evident. It is difficult to reliably differentiate openly healed cavities from active disease and other causes of lung cavitation solely based on radiological appearance. However, clinical scenario and serial imaging may give a clue as to the diagnosis. Also, as in our series, healed tuberculous cavities are usually associated with adjacent atelectasis or scarring and calcifications.

Aspergilloma

Saprophytic aspergillosis (aspergilloma) is characterised by Aspergillus infection without tissue invasion. It typically leads to conglomeration of intertwined fungal hyphae admixed with mucus and cellular debris within a pre-existent pulmonary cavity or ectatic bronchus [11,12]. Approximately 25-55% of patients with aspergilloma have a history of chronic cavitary tuberculosis. The prevalence of aspergilloma associated with chronic tuberculosis has been reported to be 11-15.3%, with haemoptysis being the most common clinical complication [6,13-15]. CT shows a mobile fungus ball, usually with air interspersed between the masses of mycelia. Also, the rounded mass is surrounded by a crescentic air shadow inside the lung cavity (air-crescent sign). Calcification of the mycelial ball occurs in some cases. The aspergilloma usually moves when the patient changes position.

Tuberculomas

Pulmonary tuberculomas can be the manifestation of both primary and post-primary TB. A pulmonary tuberculoma is a well-circumscribed caseous pulmonary nodule or mass encapsulated by multiple layers of connective tissue without surrounding inflammation. The underlying pathogenesis is postulated to be repeated extension of bronchopneumonic foci, subsequent necrosis, and re-encapsulation of its capsule. Closed healing of cavities and a rounded-off, contracted, healing tuberculous lesion are suggested as other mechanisms. Tuberculomas can be solitary or multiple and range in diameter from 0.5 to 4.0 cm or greater [6]. Typically, they are smooth or sharply defined. Calcification is found in 20-30% of tuberculomas and is usually nodular and diffuse [16].

In our study, tuberculomas were noted in 54 patients (54%), with the majority of the patients showing bilateral distribution, being clustered in the upper lobes or superior segments of the lower lobes, paralleling the distribution of other tuberculous lesions. The average size of the tuberculomas in our study was 6 mm ±1.6 mm, with none of the patients showing a tuberculoma more than a centimetre in size. Calcification is common in healed tuberculomas with the common pattern being diffuse and central. Also, patients presenting with only non-calcified tuberculomas showed other sequelae of healed tuberculosis like parenchymal fibrosis, bronchiectasis, or calcified mediastinal nodes.

Airway lesions

Bronchiectasis, tracheobronchial stenosis, and broncholithiasis

Bronchiectasis may develop as a result of tuberculous involvement of the bronchial wall and subsequent fibrosis or destruction or fibrosis of the lung parenchyma with secondary bronchial dilatation. Hatipoglu *et al.* found that bronchiectasis was seen in 71% of patients with inactive disease in high-resolution CT [8]. Bronchiectasis located in the apical and posterior segments of the right upper lobe and apicoposterior segment of the left upper lobe is highly suggestive of a tuberculous origin. In our study, bronchiectasis was noted in 77% patients, with the majority showing cystic bronchiectasis, followed by tubular bronchiectasis and a few showing varicose bronchiectasis.

Tracheobronchial stenosis may result from granulomatous changes in the tracheobronchial wall or by extrinsic pressure from enlarged tuberculous peribronchial nodes in approximately 2-4% of patients with PTB [6,17]. The left main bronchus is most frequently involved in fibrotic disease. The CT findings include concentric narrowing of the lumen, uniform thickening of the wall, and involvement of a long bronchial segment in the fibrotic stage. In our series, 4% patients showed tracheobronchial stenosis with distal collapse and fluid bronchogram. One of these patients showed involvement of the left main bronchus with complete collapse of the left lung, while in other patients, lobar bronchi were involved.

Broncholithiasis is defined as the presence of calcified material within the tracheobronchial lumen, commonly seen secondarily to a calcified peribronchial tuberculous lymph node eroding into the bronchial wall. CT shows a calcified lymph node that is either endobronchial or peribronchial and is associated with findings of bronchial obstruction, such as atelectasis, obstructive pneumonitis, or bronchiectasis.

Mediastinal lesions

Lymph node calcification

Tuberculous mediastinal lymphadenitis is a frequent manifestation of primary pulmonary tuberculosis. In the active stage, tuberculous mediastinal lymph nodes show central low attenuation and peripheral rim enhancement in CT. With treatment, the nodes first become homogeneous and finally disappear or result in a residual mass composed of fibrotic tissue and calcifications without low-attenuation areas [18]. In our series, 74% of patients showed calcified mediastinal nodes, primarily in pretracheal, paratracheal, precarinal, subcarinal, and hilar regions. Hatipoglu *et al.* [8] found that 15/34 (44%) patients with inactive pulmonary

tuberculosis showed calcified mediastinal and hilar nodes. Other common causes of mediastinal nodal calcification are sarcoidosis, silicosis, treated lymphoma, and histoplasmosis. Clinical history and associated parenchymal changes, however, indicate the appropriate diagnosis.

Pericardial tuberculosis

Tuberculous pericarditis is reported to complicate up to 1% of cases of tuberculosis. Constrictive pericarditis occurs in about 10% of patients with tuberculous pericarditis. It is characterised by fibrous or calcific constrictive thickening of the pericardium, which prevents normal diastolic filling of the heart. CT shows pericardial thickening of more than 3 mm with or without pericardial effusion. In our series, two patients (2%) showed pericardial thickening, with one showing interrupted calcification and the other showing sheet like calcification. Pericardial calcification is seen most commonly following previous trauma/surgery, episode of pericarditis, radiotherapy, infection, and connective tissue disorders [19].

Fibrosing mediastinitis

Fibrosing mediastinitis is postulated to result from chronic inflammation associated with profound fibrotic changes along the mediastinal structures due to adjacent primary granulomatous disease, either via direct infiltration from granuloma rupture or indirectly via local inflammatory processes within regional mediastinal lymph nodes. The various causes of fibrosing mediastinitis includes granulomatous diseases (such as histoplasmosis, TB, sarcoidosis), malignancy (such as bronchogenic tumour, lymphoma), trauma, and medication-induced (methysergide), IgG-4-mediated disease [20,21].

The development of fibrotic infiltrates/masses has the potential to encase and compromise mediastinal structures including the airway, oesophagus, and/or major vessels. Characteristic findings on CT or magnetic resonance imaging include soft tissue obliteration of normal mediastinal fat planes with or without encasement and invasion of adjacent structures.

The mediastinal granulomatous lymph nodes coalesce, and the development of multiple tuberculous granulomas creates both reactive fibrous changes and acute inflammatory changes in the mediastinum. The granulomas evolve into fibrosing mediastinitis when reactive changes predominate. CT findings include a mediastinal or hilar mass, calcification in the mass, tracheobronchial narrowing, pulmonary vessel encasement, superior vena cava obstruction, and pulmonary infiltrates.

Pleural lesions

Pleural sequelae include pleural thickening, which was evaluated on the basis of pleural thickness, enhancement, and calcification [22]. Fibrothorax with diffuse pleural thickening but without effusion on CT scans suggests inactivity. Chyliform or pseudochylous pleural effusion is a high-lipid non-chylous effusion and is most commonly caused by tuberculous empyema. The diseased pleura may result in an abnormally slow transfer of cholesterol and other lipids, originating from degenerated red and white blood cells, out of the pleural space, and lead to accumulation of cholesterol in the pleural fluid. CT shows a fat-fluid or fat-calcium level [23].

Pleural thickening was noted in 22 patients (22%), with the average pleural thickness being 3.8 mm (range, 3-9 mm). 8/22 (36.36%) showed pleural enhancement, while 9/22 (40.9%) showed interrupted calcifications. 2/22 patients (9.1%) showed continuous thick calcification with ipsilateral volume loss and fibrothorax.

Vascular complications

Rasmussen's aneurysm is pulmonary artery aneurysm which occurs in cavitary tuberculosis, which is caused by gradual weakening of adjacent pulmonary arterial wall. The granulation tissue replaces the adventitia and media of the vessel wall, which is replaced by fibrin, leading to thinning and pseudoaneurysm formation. Rasmussen's aneurysm was noted in 4% of our patients, with the average size being 5 mm. A review of autopsy findings in patients with a history of chronic cavitary tuberculosis showed a 5% prevalence of Rasmussen aneurysm [24]. Haemoptysis is the usual presenting symptom and may be life-threatening when it is massive.

Bronchial arteries may be enlarged in bronchiectasis associated with tuberculosis or in parenchymal tuberculosis. Bronchial arteries in patients with chronic inflammation become hypertrophied and lead to development of bronchopulmonary and arteriovenous communications. Enlarged bronchial arteries were noted in three (3%) patients.

Pulmonary arteries and veins in an area of active tuberculous infection may demonstrate vasculitis and thrombosis.

Conclusions

Pulmonary tuberculosis leads to significant morbidity, even after completion of the recommended treatment. It has multiple appalling parenchymal, airway, pleural, mediastinal, and vascular sequelae, which warrant accurate diagnosis and timely management in symptomatic cases. Radiological evaluation assumes a pivotal role in patient assessment and decision making.

Conflict of interest

The authors report no conflict of interest.

References

1. WHO. Global Tuberculosis Report 2018. World Health Organization 2018.
2. Kyu HH, Maddison ER, Henry NJ, et al. The global burden of tuberculosis: results from the Global Burden of Disease Study 2015. Lancet Infect Dis 2018; 18: 261-284.
3. Kyu HH, Maddison ER, Henry NJ, et al. Global, regional, and national burden of tuberculosis, 1990–2016: results from the Global Burden of Diseases, Injuries, and Risk Factors 2016 Study. Lancet Infect Dis 2018; 18: 1329-1349.
4. Oxlade O, Murray M. Tuberculosis and poverty: why are the poor at greater risk in India? PLoS One 2012; 7: e47533.
5. Menon B, Nima G, Dogra V, Jha S. Evaluation of the radiological sequelae after treatment completion in new cases of pulmonary, pleural, and mediastinal tuberculosis. Lung India 2015; 32: 241-245.
6. Kim HY, Song KS, Goo JM, et al. Thoracic sequelae and complications of tuberculosis. Radiographics 2001; 21: 839-858.
7. Van Dyck P, Vanhoenacker FM, Van den Brande P, De Schepper AM. Imaging of pulmonary tuberculosis. Eur Radiol 2003; 13: 1771-1785.
8. Hatipoğlu ON, Osma E, Manisali M, et al. High resolution computed tomographic findings in pulmonary tuberculosis. Thorax 1996; 51: 397-402.
9. Hermel MB, Gershon-Cohen J. Healing mechanisms of tuberculous cavities. Radiology 1954; 63: 544-549.
10. Winer-Muram HT, Rubin SA. Thoracic complications of tuberculosis. J Thorac Imaging 1990; 5: 46-63.
11. Soubani AO, Chandrasekar PH. The clinical spectrum of pulmonary aspergillosis. Chest 2002; 121: 1988-1999.
12. Ortiz-Brizuela E, Ponce-de-León A. Chronic pulmonary aspergillosis after pulmonary tuberculosis. Can Med Assoc J 2018; 190: E1171-E1171.
13. Fraser RS, Müller NL, Colman N, Pare PD. Fraser and Paré's Diagnosis of Diseases of the Chest. Vol. 1-4. WB Saunders 1999.
14. Chatzimichalis A, Massard G, Kessler R, et al. Bronchopulmonary aspergilloma: a reappraisal. Ann Thorac Surg 1998; 65: 927-929.
15. Smith NL, Denning DW. Underlying conditions in chronic pulmonary aspergillosis including simple aspergilloma. Eur Respir J 2011; 37: 865-872.
16. Lee KS, Song KS, Lim TH, et al. Adult-onset pulmonary tuberculosis: findings on chest radiographs and CT scans. AJR Am J Roentgenol 1993; 160: 753-758.
17. Leung AN. Pulmonary tuberculosis: the essentials. Radiology 1999; 210: 307-322.
18. Moon WK, Im JG, Yeon KM, Han MC. Mediastinal tuberculous lymphadenitis: CT findings of active and inactive disease. AJR Am J Roentgenol 1998; 170: 715-718.
19. O'Leary SM, Williams PL, Williams MP, et al. Imaging the pericardium: appearances on ECG-gated 64-detector row cardiac computed tomography. Br J Radiol 2010; 83: 194-205.
20. McNeeley MF, Chung JH, Bhalla S, Godwin JD. Imaging of granulomatous fibrosing mediastinitis. Am J Roentgenol 2012; 199: 319-327.
21. Tan R, Martires J, Kamangar N. Tuberculosis-associated fibrosing mediastinitis: case report and literature review. J Clin Imaging Sci 2016; 6: 32.
22. Müller NL. Imaging of the pleura. Radiology 1993; 186: 297-309.
23. Song JW, Im JG, Goo JM, et al. Pseudochylous pleural effusion with fat-fluid levels: report of six cases. Radiology 2000; 216: 478-480.
24. Santelli ED, Katz DS, Goldschmidt AM, Thomas HA. Embolization of multiple Rasmussen aneurysms as a treatment of hemoptysis. Radiology 1994; 193: 396-398.